The Holocene 16,5 (2006) pp. 705–716

Pattern and timing of sediment infill at glacier-fed Mud Lake: implications for lateglacial and Holocene environments in the Monashee Mountain region of British Columbia, Canada

K.R. Hodder,[1]* J.R. Desloges[2] and R. Gilbert[1]

([1]Department of Geography, Queen's University, Kingston, Ontario K7L 3N6, Canada; [2]Department of Geography, University of Toronto, Toronto, Ontario M5S 3G3, Canada)

Received 8 June 2005; revised manuscript accepted 3 February 2006

Abstract: The Holocene sedimentary infill of proglacial Mud Lake, British Columbia, Canada, was investigated using 3.5 kHz acoustic sub-bottom profiling and sediment samples. The sediment infill is a mixture of silt and clay and is divided into five stratigraphic units: massive silt (Unit 1), weakly laminated silt with very fine sand beds (Unit 2), weakly laminated silt with rippled beds of fine sand (Unit 3), weakly laminated clay with very fine sand laminations (Unit 4) and silt–clay varves (Unit 5). Acoustic reflectors correlate with stratigraphic unit boundaries. Annual accumulation rates were estimated for six age/depth intervals: prior to 9.6 kyr cal. BP, accumulation rates were very high – on the order of several centimetres per year. Early to middle Holocene sediment inputs (9.6–3.6 kyr cal. BP) were variable but low, ranging from 0.3 mm/yr to 1.2 mm/yr. The late Holocene (most recent 3.6 kyr) shows annual accumulation rates that generally exceed 2 mm/yr. Surface sediment reveals a mean of 4.3 mm/yr over the last 20 years. These results are consistent with regional Holocene chronologies and long-term paraglacial succession: (1) maximum sediment and meltwater availability and minimum stabilization by vegetation following Fraser deglaciation replaced by (2) less meltwater and sediment availability during the Hypsithermal, and (3) more stabilized sediment during the early and mid Holocene. Renewal of glacial activity, particularly in the late Neoglacial, has led to increased rates of accumulation in Mud Lake. Despite the contrasting geologic setting of Mud Lake in the Omineca belt, contemporary sediment yield is consistent with the trend of sediment yield with glacier cover in lakes of the adjacent Foreland belt.

Key words: Glacier-fed lake, acoustic records, sediment yield, varves, Holocene climate, British Columbia, Canada.

Introduction

Sedimentary sequences from glacier-fed lakes in the Canadian Cordillera are potentially rich archives of lateglacial and Holocene environmental change, recording variability in climatic (Leonard and Reasoner, 1999), hydrologic (Gilbert *et al*., 1997) and geomorphic conditions (Desloges and Gilbert, 1994a,b; Desloges, 1999). These lakes can provide a continuous record of the changing sedimentary environment and may record abrupt changes in the quantity and composition of sediments delivered during and after the transition from lateglacial to Holocene environments (Desloges and Gilbert, 1995; Eyles *et al*., 2000). While the number of glacilacustrine sediment chronologies in the Canadian Cordillera is growing rapidly, significant gaps exist in the Omineca and Intermontane tectonic belts (see below and Figure 1) where regional bedrock and climate may differ from those of previous investigations. Filling these gaps is important for developing comprehensive regional-scale models of Holocene environmental change. The objectives of this study are to (1) examine the spatial and temporal pattern of changing sedimentation in a lake that represents the drier (more continental) and dominantly metamorphic lithology of basins in eastern British Columbia; (2) infer environmental conditions that lead to these

*Author for correspondence (e-mail: kr.hodder@utoronto.ca)

10.1191/0959683606hl965rp

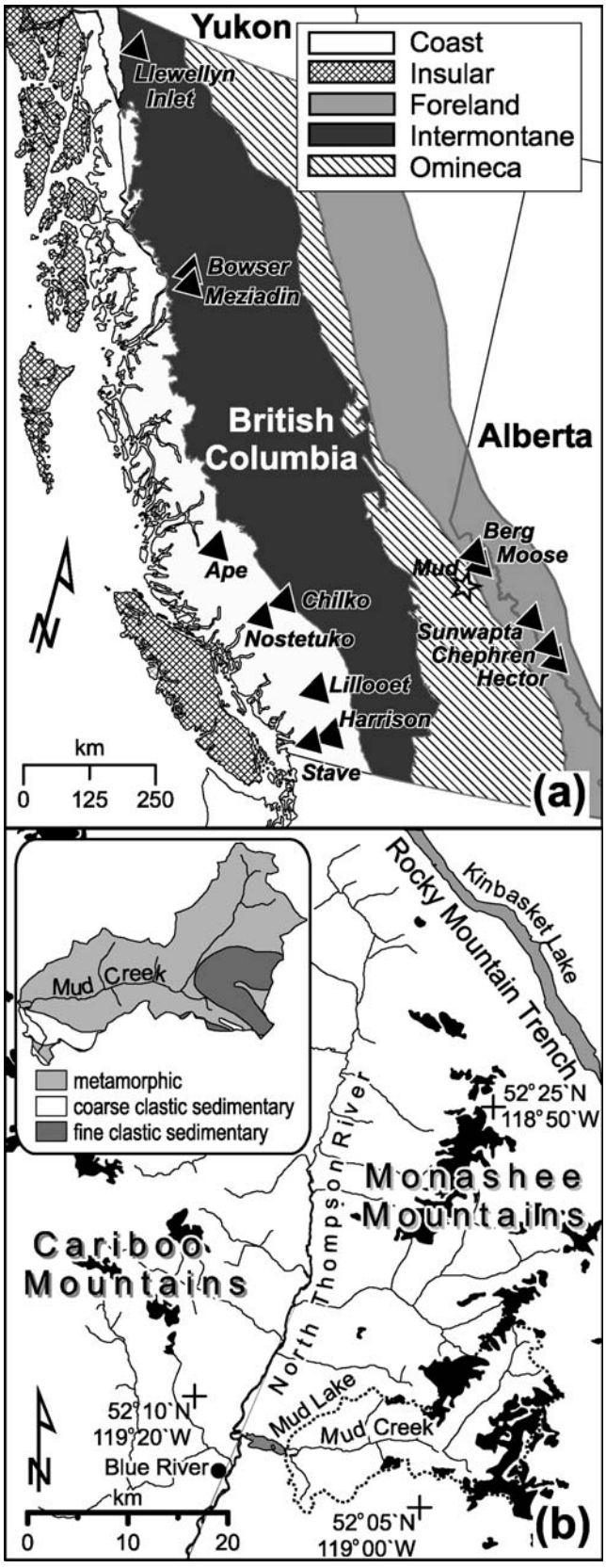

Figure 1 Map showing (a) location of Mud Lake (star) and other lakes referenced in this study (triangles), along with tectonic belts of British Columbia (modified from Wheeler and McFeely, 1991) and (b) regional map of the North Thompson River (glaciers shown in black); drainage basin of Mud Creek in dashed outline; inset map of watershed geology adapted from Höy *et al*. (1994)

patterns, and (3) compare the accumulation variability with other regional patterns observed in lakes throughout the Canadian Cordillera.

Study area and field methods

Mud Lake lies within the Omineca belt of the Canadian Cordillera (Figure 1a), a zone of mixed (although dominantly metamorphic) rocks. Regional bedrock geology maps prepared by Höy *et al*. (1994) show about 80% of the Mud Lake basin is metamorphic pelites and about 20% is clastic mudstones and shales (Figure 1b). However, about 64% of the contemporary glacial ice sits atop pelite and the balance (~36%) overlies clastic rocks.

Most of the inflow to Mud Lake is from Mud Creek at the east end of the lake, providing runoff from a 257 km^2 drainage basin (Figure 1b). Elevation in the basin ranges from 678 m a.s.l. at the lake to approximately 2900 m a.s.l. Niche and small cirque glaciers occupy 22.1% of the basin by area, and smaller snow patches persist throughout the summer at the highest elevations. There are no lakes upstream of Mud Lake that would otherwise filter coarse particles reaching the lake via Mud Creek. Mud Lake drains into the North Thompson River via a 0.9 km channel at the west end of the lake. The lake is 4 km long, averages 990 m in width and 27 m in depth (Figure 2). Maximum depth is 54 m. Subaqueous sills northwest and south of Smoke Island (27 m and 3 m below summer water level, respectively) separate the lake into proximal and distal basins.

Over 25 km of acoustic survey was conducted using a Datasonics Chirp-II acoustic profiler. Water depths and depths into the sediment column assume a sound velocity of 1430 m/s in water (Marczak, 1997). Sediments were recovered in two vibracores (cf. Smith, 1998; Fisher, 2004) 12.6 m (VC1) and 9.9 m long (VC2) from ice cover during February 2000 and at 25 other sites using an Ekman box corer during August 2000 (Figure 2). A single GPS receiver was used to position coring sites and acoustic survey tracks (the latter at 10 s intervals).

Ekman box cores were subsampled in the field with an 80 mm diameter cylinder pushed into the sediment to preserve the sediment surface and structures of the upper 10–15 cm. Residual sediment was bagged for bulk particle size analysis. The cores were split in the laboratory where the working half was logged (Schnurrenberger *et al*., 2003) and photographed. Stratigraphy of the two vibracores was identical, so VC1 was selected for detailed analysis of particle size, organic content and lithostratigraphy at 5 cm intervals and major stratigraphic breaks. Sediment samples were chemically dispersed in a 0.5% sodium hexametaphosphate solution for 24 h and mechanically dispersed for five minutes in an ultrasonic bath prior to particle size analysis. A Sedigraph-5100 was used to measure particle size distribution, and the loss-on-ignition method was used to estimate organic matter content (Dean, 1974). AMS ^{14}C dating of available wood fragments, identification of tephra layers using an electron microprobe, and varve counting were used to establish a chronology of sedimentation. All ^{14}C dates, including those reported elsewhere for tephra, were calibrated with OxCal 3.10 (Bronk Ramsey, 1995, 2001) using the calibration data set from Reimer *et al*. (2004). Dates are also reported here in calibrated years BP based on the 1-sigma range midpoint (in parentheses), or weighted average of the 1-sigma midpoints in the case of multiple ranges, except where otherwise noted.

Results

Lithostratigraphy

The stratigraphic sequences at the core sites generally consist of massive to weakly laminated silt, and strongly laminated silty clay. The dates from organic fragments and tephra

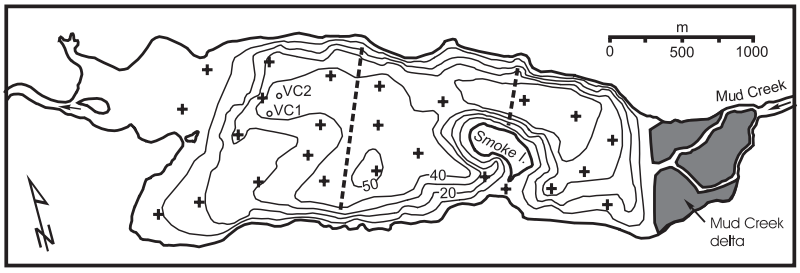

Figure 2 Bathymetry of Mud Lake determined from 25 km of sub-bottom acoustic survey, assuming sound velocity in water value of 1430 m/s. Isobath interval 10 m. Also shown are locations of vibracores (VC1, VC2; circles), Ekman box cores (crosses) and the acoustic profiles presented in Figures 5 and 6 (dashed lines)

(Figure 3a) indicate that VC1 preserves nearly all of the Holocene record. Median particle size (D_{50}) shows an overall fining-upward trend (Figure 3b), largely the result of a greater clay fraction (at the expense of the silt fraction; Figure 3c). Organic matter content (Figure 3d) is consistently low through most of the record (near 3.5%). Based on the particle size distribution, organic content and bedding features, the sequence can be subdivided into five lithostratigraphic units (Figure 3a). Unit 1, below 10.4 m, is massive silt. Organic matter content is highest in this unit, reaching a maximum near 6%. Macrofossil (twig) samples recovered at 12.53 m and 10.85 m date to 8580 ± 70 ^{14}C BP or 9480 (9555) 9630 cal. BP (TO-8838) and 5880 ± 60 ^{14}C BP or 6630 (6710) 6790 cal. BP (TO-8839), respectively. With the exception of a 2 cm thick bed of tephra at 11.86 m identified as Mazama, there are no bedding structures observed in this unit. Mazama tephra has been dated to 6730 ± 40 ^{14}C BP or 7565 (7600) 7655 cal. BP by Hallett *et al.* (1997). D_{50} in Unit 1 has an overall mean of 8.3 μm, and the upper boundary of this unit is marked by a sharp contact where sand content increases by 7.1% at 10.4 m.

Unit 2, between 10.40 m and 7.59 m, is weakly laminated silt with occasional very thin beds of very fine-sand. Silt laminae consist of millimetre-scale lighter colour (10YR 8/4 to 5YR 6/2) beds in centimetre-scale sets alternating with darker (5 YR 3/2) fine-sand beds or poorly bedded sequences. Fine-sand beds have sharp lower contacts, fine upwards diffusely into silt, and no bedding structures are visible within. Mean D_{50} is 11 μm within Unit 2. A 1.5 cm thick tephra bed identified as St Helens Yn, occurs at 7.62 m. The St Helens Yn tephra has been dated to 3360 ± 65 ^{14}C BP or 3480 (3595) 3690 cal. BP by Vogel *et al.* (1990).

In Unit 3, between 7.59 and 5.60 m, weakly laminated silt appears similar in structure and colour to that in Unit 2. However, the silt is interrupted by thin beds of fine sand that generally fine upwards from sharp lower contacts. Many fine-sand beds preserve distinct ripple structures composed of millimetre-scale light coloured (10 YR 7/2) laminae alternating with darker coloured (5 YR 3/2) beds that are collectively of centimetre-scale. The maximum thickness of any group of ripple-structure beds is 4.5 cm. D_{50} is most variable in this unit, varying between 2 μm and 30 μm over intervals as short as 5 cm. Variation in median particle size corresponds with bedding structure: highest values are found within the base of the fine-sand beds, while lowest values are found in the silt just below the fine-sand beds. Organic content is lowest in this unit with a mean of 2%. The upper boundary of Unit 3 corresponds with an abrupt reduction in D_{50}.

In Unit 4, between 5.60 m and 2.60 m, weakly laminated clay is interrupted by laminations (rare very thin beds) of very fine-sand in places. Many of these sand beds fine upwards diffusely into the overlying clay. On average, Unit 4 has the highest proportion of clay sediment ($\bar{x} = 65\%$) and a correspondingly low overall D_{50} ($\bar{x} = 2.6$ μm). It also has the lowest variability in D_{50} of any unit. Organic content has a mean of 3.4% and shows no trend with depth.

Unit 5, the uppermost 2.60 m, consists of regularly alternating couplets of fine to medium silt that grade diffusively into clay caps, which in turn have abrupt upper contacts with the overlying silt. Below 1.24 m, laminations are present, but couplet structure is considerably less distinct. In the upper 2 m, the proportion of clay to silt is consistent at 3:2. D_{50} has an overall mean of 3.1 μm. Sand comprises $< 1\%$ of the unit by mass, and individual sand particles are rarely visible within laminae. Each lamina also has a characteristic colour. Relatively thick light coloured (7YR8/2) silt laminae alternate with thinner, darker (7YR6/2) clay laminae. The average thickness of the couplets in the upper 1.24 m of sediment is 4.2 mm ($n = 293$; $\sigma = 1.8$).

^{137}Cs determinations were made on samples from the upper portion of the core to test the assumption that rhythmites in Unit 5 are varves. Although there was insufficient sediment mass to finely resolve each varve year, three sediment samples – each combining several possible annual varves – were selected based on varve counting. The lower sample (25–32 cm) and upper sample (5–15 cm) were selected to represent pre-1954 and post-1963 minimums in atmospheric input of ^{137}Cs, respectively (Blais *et al.*, 1995). ^{137}Cs concentrations of over 42 Bq/kg were noted for the middle sample (15–25 cm) which most likely contains the 1954–1963 peaks of ^{137}Cs production. This compares with concentrations below detection limit (< 12 Bq/kg) below and only slightly above detection limits (17 Bq/kg) in the overlying sediment. From the surface to 18.5 cm, there are 40 laminae, and thus the rhythmites are considered varves. Although they compose the upper 1.24 m of sediment, a continuous sequence of varves can only be traced from the surface to 0.49 m depth (129 varves) where disturbance interrupts the sequence. The disturbance is the result of post-sampling division of the core pipe for transport, as it is not present at the same depths in core VC2.

Spatial trends

Bulk samples from Ekman box cores were used to determine the spatial pattern of sedimentary structures ($n = 18$) and particle size properties ($n = 25$). In the proximal basin, the mean sand fraction of bottom sediment exceeds 25%. Beds show sharp (likely erosive) lower contacts and individual sand beds range in thickness from < 1 to 4 cm, especially near the delta. Varves are clearly recognized only at positions greater than 1 km from the delta, so spatial patterns of sedimentary structures are not interpreted in the proximal basin.

Spatial patterns in sedimentary structure and particle size show a consistent trend with (a) distance from the Mud Creek delta and (b) laterally from the north and south sides of the lake. The proximal basin has an average D_{50} of 24.4 μm ($\sigma = 2.0$) compared with 3.40 μm ($\sigma = 0.7$) in the distal basin (Figure 4a). The large difference reflects the division of the lake

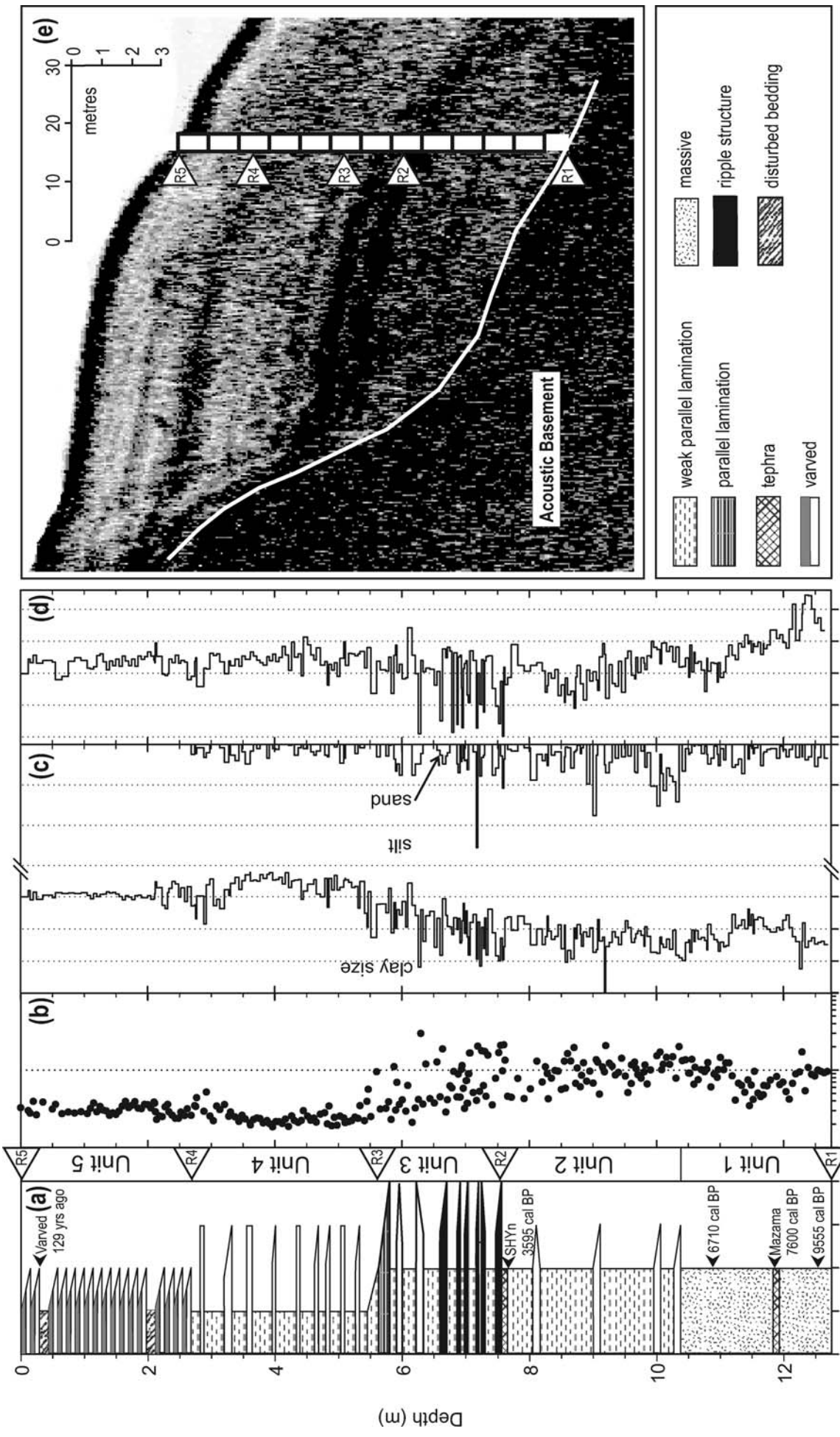

Figure 3 Analysis of VC1 at 5 cm intervals for (a) lithostratigraphy and sediment units 1 through 5; (b) median particle size; (c) percent fraction of sand, silt and clay particles and (d) percent organic content by loss on ignition. (e) Acoustic record from the location of vibracore VC1 (superimposed in white with 1 m subdivisions). Triangles represent acoustic reflector labels 1 through 5. Where lithostratigraphic units are thin (eg, sand laminations), vertical dimension has been emphasized for clarity (proportional, but not to scale)

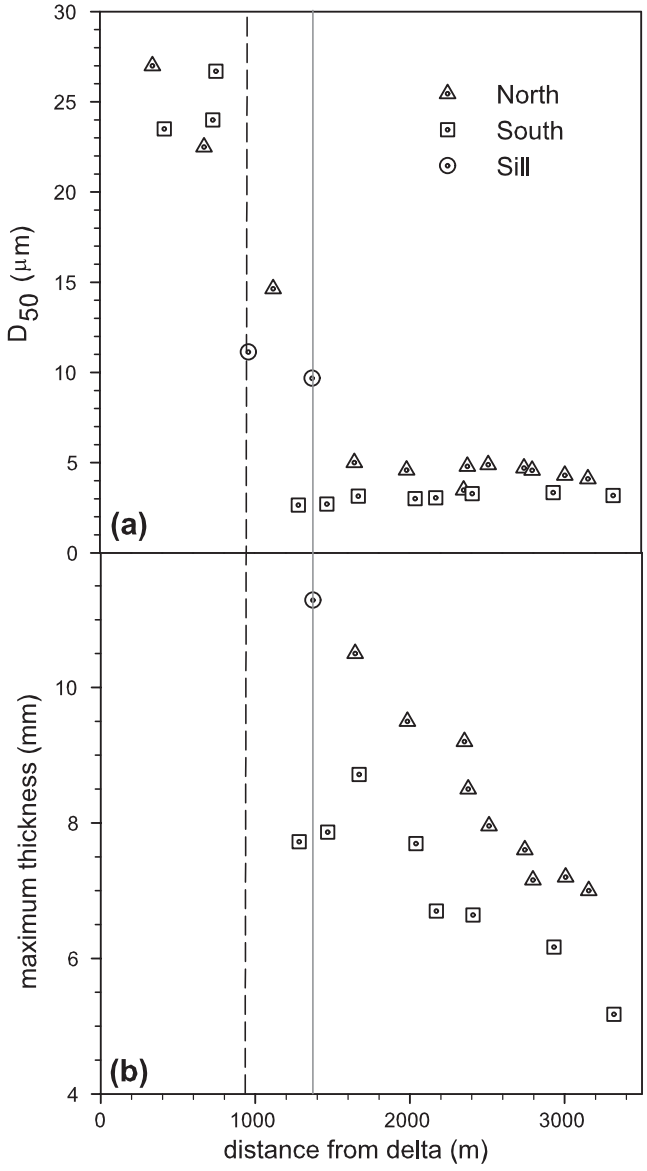

Figure 4 Spatial trend in (a) median particle size (D_{50}) and (b) maximum couplet thickness (mm), plotted by distance from Mud Creek delta, and approximate position of north sill (solid line) and south sill (dashed line)

into proximal and distal sub-basins by the sills. Median particle size measured on the sills is intermediate to the values from each basin at 10.4 μm, and shows intermediate variability ($\sigma = 1$). D_{50} on the north side of the distal basin is coarser ($\bar{x} =$ 5.0 μm, $\sigma = 0.5$), compared with the south side ($\bar{x} =$ 2.8 μm, $\sigma = 0.3$; Figure 4a).

Maximum varve thickness in the distal basin decreases by about 5 mm over a distance of 2100 m (Figure 4b). Minimum varve thickness does not show any consistent trend with distance from the Mud Creek delta or north/south sides of the lake. Although no trend is noted with distance from the delta, mean varve thickness on the north side of the lake is greater and more variable. Mean varve thickness on the north side is 5.0 mm (max = 11.3, $\sigma = 0.8$), compared to 3.6 mm (max = 8.5, $\sigma = 0.5$) on the south side (Figure 4b).

The combined structure and particle size results suggest that proximal–distal trends are partly controlled by bottom topography, as turbidity currents are known to follow the lowest areas of the lake floor and to be impeded by cross-lake sills (Chikita *et al.*, 1996) Lake-sill impediment of turbidity currents has also been inferred in lakes elsewhere (eg, Gilbert *et al.*, 1997). Turbidity current activity in the proximal basin is consistent with the coarser sediments located there and might contribute to the difficulty in proximal varve identification if the currents were erosive, curbed silt and clay deposition (resulting from higher ambient energy) or both. Within the distal basin, varves formed farther from the delta are thinner and less variable than those formed more proximally. This is consistent with sediment delivery via overflow or shallow interflow allowing sediment to disperse over the lake. These surficial currents are deflected northward by the combined influence of the Coriolis effect, deflection by Smoke Island and the prominent sill (and narrows) to the south. This role of the Coriolis effect in the distribution of sediment has also been reported by Smith *et al.* (1982), and Pickrill and Irwin (1983).

Sub-bottom acoustic records

In the proximal basin, the dominance of sandy sediment within about 250 m of the delta limited acoustic penetration to a maximum of 2 m. A single acoustic facies is recognized in the proximal basin on the basis of geometry, strength and continuity of reflectors (Figure 5). This basin is characterized by high-amplitude, parallel reflectors with submetre spacing. Minimal sediment accumulation has occurred on the side slopes, and the facies has a mean thickness of 19 m (decreasing distally). Reflectors terminate discordantly with the acoustic basement, and reflectors diverge northward. The magnitude of divergence of reflectors increases with distance from the Mud Creek delta. At 350 m from the delta, there is no divergence, and bathymetry of the lake floor is uniform from north (right) to south (left). At 1100 m from the delta (near the edge of the proximal basin), reflectors are divergent and bathymetry of the lake floor is 9 m shallower on the north (right) side.

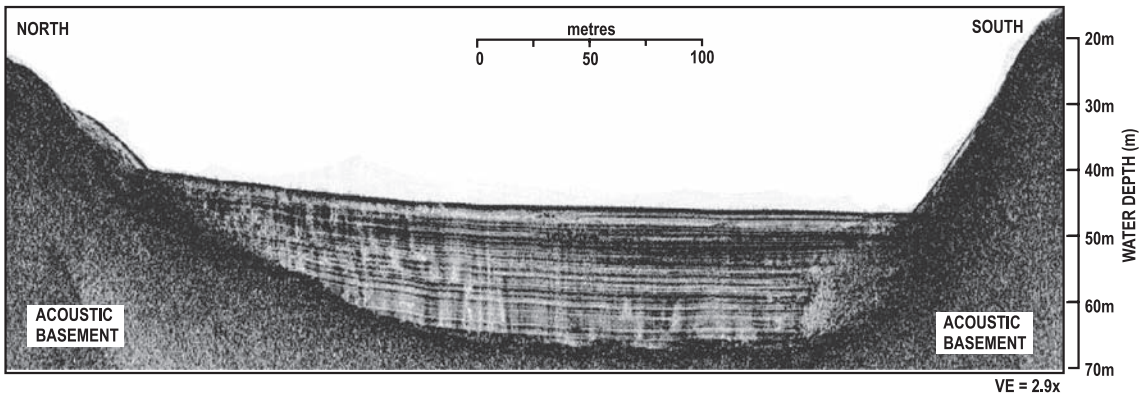

Figure 5 Sub-bottom acoustic record from the proximal basin. For location, see Figure 2. Water depths and depths into the sediment column assume a sound velocity of 1430 m/s in water

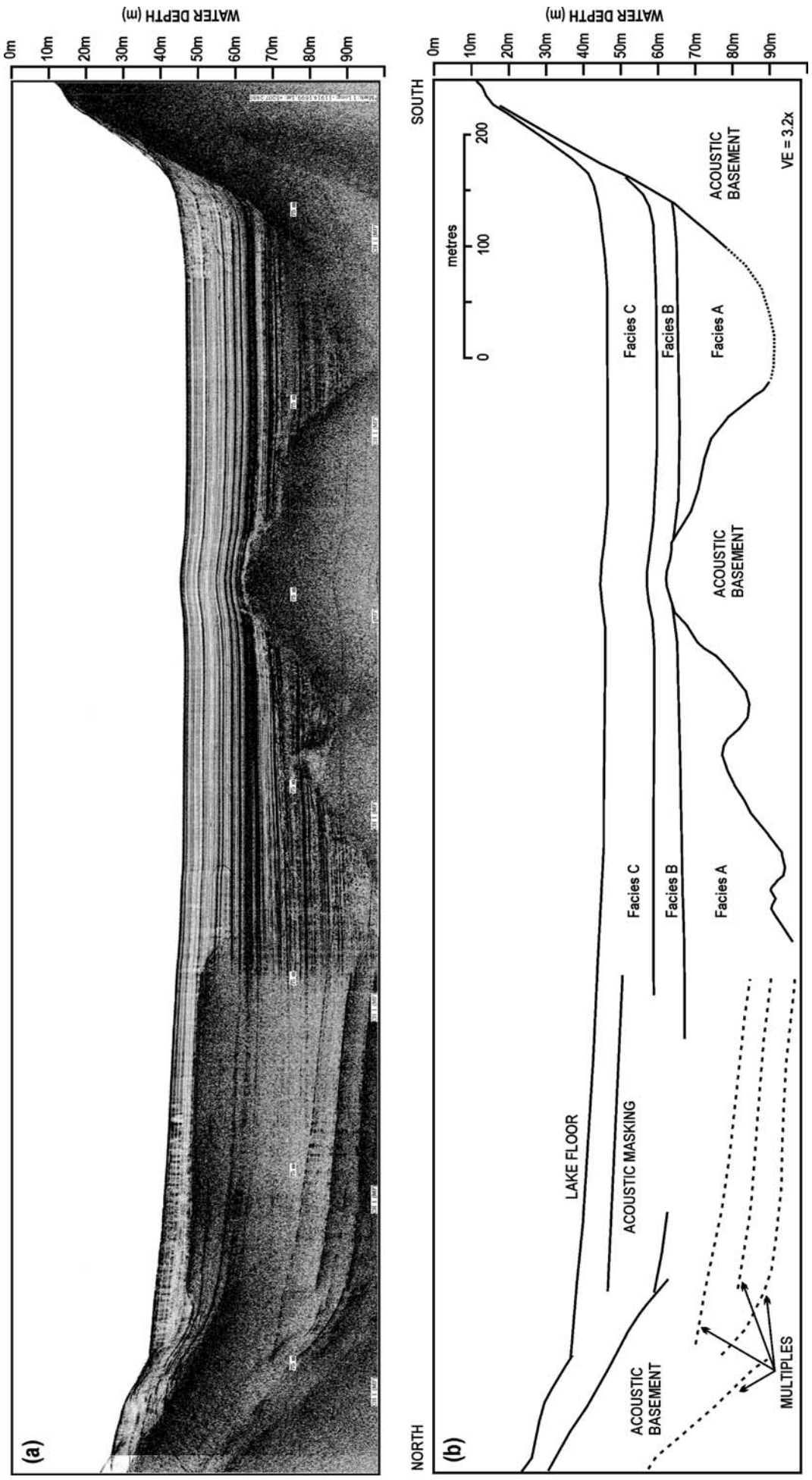

Figure 6 Sub-bottom acoustic record from distal basin showing the acoustic facies described in the text. For location, see Figure 2. Water depths and depths into the sediment column assume a sound velocity of 1430 m/s in water

Elsewhere in the lake, the acoustic record reveals that the maximum thickness of fine sediment (silt and clay) is 56 m and occurs near the centre of the lake in the distal basin. The thickest and deepest sediment lies discordantly over a hummocky acoustic basement, interpreted as bedrock or ice-contact glacial sediment. Apart from the acoustic basement surface, there are no unconformities in the acoustic record. Little sediment has accumulated on the side slopes of the basin in comparison with the basin floor, but there is no evidence of sediment slumping except near the delta (cf. Gilbert and Desloges, 1992). The foreset beds of the delta have a slope of about 4° and at least seven slumps are visible near the delta toe (cf. Desloges and Gilbert, 1994b). Maximum height of the slumped sediment mounds is about 3 m.

Three acoustic facies can be recognized in distal basin sediments based on the geometry, strength and continuity of the reflectors (Figure 6). The lowest unit, Facies A, has a maximum thickness of 39 m and discordantly overlies the acoustic basement. Subparallel reflectors in packages of three or four, spaced about 1 m apart, are separated by structureless zones 3–5 m thick. Reflectors in Facies A have irregular surfaces in detail.

A high amplitude, ubiquitous reflector separates Facies A from Facies B above. Facies B is distinguished by high amplitude parallel reflectors spaced about 2 m apart. Its mean thickness is 8 m, decreasing distally. Reflectors terminate concordantly with the surrounding acoustic basement, and reflectors diverge northward. This thickening by up to 30% on the north side of the distal basin is somewhat less than, although comparable with, the cross-lake difference in varve thickness (Figure 4b) ascribed to the Coriolis effect.

Facies C conformably overlies Facies B (Figure 6) and laps against the acoustic basement as it rises around the shores of the lake. Facies C averages 11 m in thickness and is characterized by numerous low to moderate amplitude parallel reflectors spaced less than 1 m apart. Acoustic masks are common throughout this facies, particularly along the north shore of the lake, and they are likely caused by gas in the sediments (Figure 6). As in Facies B, reflectors terminate concordantly with the surrounding acoustic basement and are divergent northward.

The acoustic records reveal lake-wide patterns of sedimentation, and the cores provide calibration. In addition to the sedimentary record of particle size distribution, central tendency and lithostratigraphy for vibracore VC1, Figure 3 (panel e) shows the acoustic record collected near the core. Acoustic reflectors correlate with anticipated changes in acoustic impedance, such as at the sediment/water interface (marked R5) and at the acoustic basement (marked R1; interpreted as bedrock or ice-contact glacial sediment). The total sediment thickness above the acoustic basement ($\sim$ 13 m) closely matches the refusal depth for the vibracore (12.74 m) suggesting near-complete sediment recovery.

Figure 3 also illustrates that strong acoustic reflectors coincide with stratigraphic unit boundaries and, in particular, abrupt changes in the particle size distribution measured in core sediment. For example, reflector R2 at 7.6 m coincides with the transition from weakly laminated silt (Unit 2) to weakly laminated silts with thin beds of fine sand (Unit 3). R2 correlates more precisely with a sand content change from 0% at 7.6 m to $>5\%$ at 7.5 m, a three-fold increase in median particle diameter (from 7.0 μm to 21 μm) and a three-fold reduction in organic content (from 3.2% to 1.0%) over the same interval.

Reflector R3 at 5.6 m coincides with a transition from weakly laminated silts with thin beds of fine sand (Unit 3) to weakly laminated clay with occasional fine sand laminations (Unit 4). Median particle diameter drops from 10 μm at 5.6 m to 2.5 μm at 5.55 m. Over the same interval, sand content drops from 1.5% to zero, while organic content jumps from 2.3% to 4.0%.

Reflector R4 at 2.6 m coincides with a transition from weakly laminated clay with occasional fine sand laminations (Unit 4) to regularly alternating couplets of fine to medium silt grading diffusively into clay caps (varves; Unit 5). Median particle diameter drops from 4.5 μm at 2.7 m to 3.1 μm at 2.6 m. Sand content drops from 1.5% to zero over the same interval. No significant change in organic content coincides with reflector R2.

Interpretation

Annual accumulation rates were estimated in core VC1 for six age/depth intervals obtained using two dating methods: radiocarbon dates (from both tephra and macrofossils) and varve counting (Figure 7). The precise timing of deglaciation is difficult to determine, but Fulton (1984) indicates deglaciation commenced about 13 kyr ^{14}C BP (minimum 15.1 kyr cal. BP), and Osborn and Luckman (1988) suggest ice retreated to near-present limits prior to 10 kyr ^{14}C BP (*c.* 11.5 kyr cal. BP). A more specific local date for the start of deglaciation in the Mud

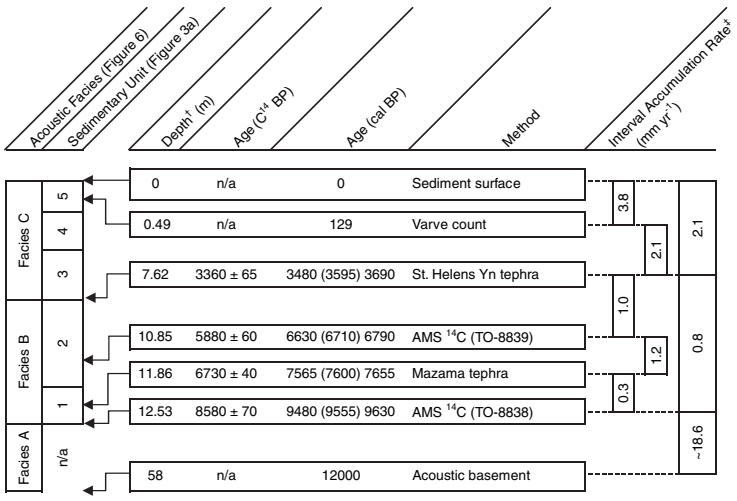

Figure 7 Accumulation rate estimated for intervals between age markers for core VC1. Not to scale. †Depth to base of unit; ‡based on interval depth and calibrated age (except Facies A; see text). The influence of 1-sigma calibrated age ranges are also omitted, as they do not significantly affect sedimentation rate estimates

Lake drainage basin has not been reported, but 12 kyr cal. BP is adopted here to represent the timing of significant ice withdrawal from major valleys. Regardless of precisely when deglaciation commenced in the study area, over 39 m of sediment accumulated in the distal basin prior to the basal date (VC1) of *c*. 9.6 kyr cal. BP. Interpolating a mean accumulation rate for the prior period is problematic given uncertainty over the timing of deglaciation. However, the rate must have been high, easily on the order of centimetres per year even accounting for uncertainty in the date of deglaciation by as much as ± 1 kyr. This was followed by a period of much lower annual accumulation during the early Holocene (0.3 mm/yr), and a modest increase in annual accumulation (> 1.2 mm/yr) between 7.6 and 6.7 kyr cal. BP. An extended period in the mid Holocene (6.7 through 3.6 kyr cal. BP) is characterized by a similar annual accumulation rate of 1.0 mm/yr. Finally, the late Holocene (most recent 3500 years) shows a return to higher annual accumulation rates (over 2.1 mm/yr). In the upper 1.24 m of sediment, 293 discontinuous varves have an average accumulation rate of 4.3 mm/yr, and 129 continuous varves have an average accumulation rate of 3.8 mm/yr. Throughout the entire distal basin, Ekman box cores indicate a mean of 4.3 mm/yr during the last 20 years, and 4.8 mm/yr during the most recent decade.

Parallel-stratified and discordant reflectors are interpreted as deposition dominated by turbidity currents emanating from Mud Creek in the proximal basin, and deposition dominated by overflow currents at points furthest into the proximal basin. This is consistent with observations of progressively thicker sediment deposits on the north side of the proximal basin at increasing distances from the delta (Wright and Nydegger, 1980; Smith *et al*., 1982). Sand, possibly deposited by turbidity currents, obscures acoustic penetration in the area nearest the delta. Turbidity currents travelling farther into the proximal basin create near-uniform, horizontal deposits near the delta. Coriolis deflection has an inverse relationship with current velocity (Hamblin and Carmack, 1978), and turbidity currents are normally significantly faster than interflows or overflows (0.3 m/s is typical; Gilbert and Shaw, 1981; Weirich, 1986). Therefore, turbidity currents would be less deflected by the Coriolis effect and result in deposits with less preferential thickening than overflows or interflows. At points furthest into the proximal basin, deposition is dominated by overflow or interflow processes that lead to greater sediment thicknesses on the north side of the lake, and these currents subsequently pass into the distal basin.

Similar in appearance to those in the proximal basin, the assemblage of parallel-stratified and discordant reflectors that dominate the lower acoustic Facies A in the distal basin are interpreted as deposits in a glacially proximal lacustrine environment. The discordant nature of the reflectors in Facies A, combined with their parallel nature, suggests deposition by energetic turbidity underflows as reported by Desloges and Gilbert (1998) and Eyles *et al*. (2000). Desloges (1999) noted horizontally stratified silt and sand in a basal unit in nearby Moose Lake and similarly interpreted them to be formed in an ice contact lake as glaciers retreated from the lake into the drainage basin. At even larger scales, Eyles and Mullins (1997) interpreted thick chaotic sequences of silt, sand and gravel in the lower seismic facies of Shuswap Lake of the South Thompson River as deposition in an ice-frontal lake during late Wisconsinan deglaciation. Thin reflector packages in Facies A separated by thicker structureless zones suggest sediment was delivered in episodic, high-magnitude pulses over a short interval in which deglaciation of the basin was rapid and abundant loose sediment was available. The lack of any preferential thickening further suggests deposition by relatively high velocity currents with little or no deposition from slower overflow or interflow currents (compare proximal basin acoustic facies). This was complete prior to 9.6 kyr cal. BP.

Facies B, captured in vibracore sampling, represents the lowest annual accumulation rate averaging 0.8 mm/yr (Figure 7). This is interpreted to represent a significant decline in available sediment delivered from the basin and is most likely related to the reduction or disappearance of headwater glaciers during the early and middle Holocene.

Facies C, also captured in vibracore sampling, indicates an early dominance of suspension (silt and clay) deposits interspersed with frequent turbidity current (sand) deposits beginning around 3.6 kyr cal. BP (Unit 3; Figure 7). These deposits suggest a return to more variable and higher discharges from Mud Creek and possible mobilization of sand that had accumulated on the delta during the Hypsithermal. Varved sediments, with no record of turbidites, form the most recent deposits over the last 129 years (Unit 5; Figure 7). The varved section of Facies C represents a mean annual accumulation rate of at least 3.8 mm/yr. The much less strongly layered earliest portion of Facies C represents a lower rate of annual accumulation that is near 2 mm/yr.

Overall, the observed change in accumulation rate is consistent with long-term paraglacial succession: maximum sediment and meltwater availability and minimum stabilization by vegetation following Fraser deglaciation replaced by less meltwater and sediment availability during the Hypsithermal and more stabilized sediment during the early and mid Holocene. A renewal of glacial activity during the Neoglacial period, particularly in the late Neoglacial, has led to increased rates of accumulation in Mud Lake.

Discussion

Evidence for lateglacial ice retreat and Holocene climate change in the headwater regions of the North Thompson River is preserved in the sediments of Mud Lake. Terrestrial evidence for the pattern of glaciation is limited, and few studies have highlighted the nature of late Pleistocene deglaciation and Holocene glacier fluctuations in the upper Columbia and Thompson rivers (Duford and Osborn, 1978, 1980; Luckman *et al*., 1987). The Monashee Mountains, which flank the west side of the Rocky Mountain Trench and separate the Columbia and Thompson drainages (Figure 1), was a primary accumulation region for Cordilleran ice. Erosional streamlining and lineations in local bedrock show that Wisconsinan ice flowed away from this mountain axis, resulting in westward flow through the Mud Lake drainage basin, coalescing in the North Thompson River valley and then southward from there.

Mud Lake records the early phase of deglaciation starting prior to *c*. 9.6 kyr cal. BP. The size and extent of the lake during early retreat is not known. A raised fan delta at the outlet of Hellroar Creek (elevation 760 m a.s.l.) in the confined reaches of the North Thompson River, 3 km north of Mud Lake, suggests a brief period of ice damming – possibly extending south from there into the main valley around Blue River. While there is no strong geomorphic evidence, the ice dam may have occurred several kilometres further south where westward-flowing ice from Froth Creek and Finn Creek drainage basins may have briefly blocked the valley to the 760 m a.s.l. level. The earliest phases of this ice-frontal lake were probably coincident with the onset of turbidite deposition in Mud Lake around 11 kyr BP (cf. Alley, 1980). Downwasting

of the ice dam in the main valley would have been rapid, and the current extent of Mud Lake was probably defined early during deglaciation. The lower acoustic package indicates that the pace of retreat was irregular and sediment supply uneven. Desloges (1999) estimates that Moose Lake in the nearby upper Fraser Valley was ice proximal or even ice dammed just before *c*. 10.3 kyr cal. BP (9120±80 ^{14}C BP). Leonard and Reasoner (1999) indicate lakes in the upper Bow River drainage about 100 km due east of Mud Lake were also receiving large quantities of ice-proximal sediment until at least *c*. 11.7 kyr cal. BP (10.1 kyr ^{14}C BP).

Cirque glaciers in the upper Mud Creek drainage basin were examined in air photographs, which reveal at least two older forest-covered moraines with morphologies and positions similar to the early Holocene Harper Creek moraine examined by Duford and Osborn (1978) at Trophy and Raft Mountains, approximately 80 km south of Mud Lake. They found Mazama ash in moraine-top soils, suggesting either an early Holocene advance (Crowfoot equivalent?) or a pause in the retreat of late Wisconsinan ice. Alley (1980) argues that this moraine type is older than *c*. 8.9 kyr cal. BP (7985±125 ^{14}C BP) but younger than *c*. 12.9 kyr cal. BP (11300±110 ^{14}C BP). We cannot confirm this for the upper Mud Lake drainage basin, but the morphologic evidence is compelling. Lateglacial and early Holocene glacier activity would have lead to development of the lowermost acoustic package.

The early and middle Holocene was characterized by direct delivery of sediment from the upper basin via the fully integrated drainage network of Mud Creek. No intermediate storage appears to have occurred, thus Mud Lake sediments record continuous changes. Leonard and Reasoner (1999) used clastic and organic lake sediments to bracket the early–middle Holocene period starting *c*. 11.5 kyr cal. BP (10 kyr ^{14}C BP) and ending between 6.6 kyr cal. BP (5.8 kyr ^{14}C BP) and 4.2 kyr cal. BP (3.8 kyr ^{14}C BP). This Hypsithermal period was characterized by much warmer and drier conditions throughout the eastern Cordillera. However, timing is thought to be time transgressive, starting later and ending earlier in the higher elevation and more northerly sites. Our results suggest warmer and drier conditions, probably with the disappearance of headwater cirque glaciers, persisted to at *c*. 3.6 cal. BP at Mud Lake.

At about 3.6 kyr cal. BP, accumulation rates increased, as did the frequency of sand laminae indicating higher energy deposits. Desloges (1999) noted the onset of thicker and better-defined varves (but no sand) in Moose Lake sediments 4100 varve years ago. An increase in sediment delivery and greater seasonal contrast in sediment type (silt–clay couplets) are most likely due to an increase in the supply of sediment and greater variability in seasonal discharges – both directly related to increasing glacier activity in the upper basin. While 'Little Ice Age' moraines dominate many of the headwater cirque glaciers here, and regionally (cf. Luckman *et al*., 1987 for the nearby Premier Range), it is likely that neoglaciation over the last few millennia has resulted in repeated minor advances and retreats. Karlstrom and Osborn (1992) have demonstrated that

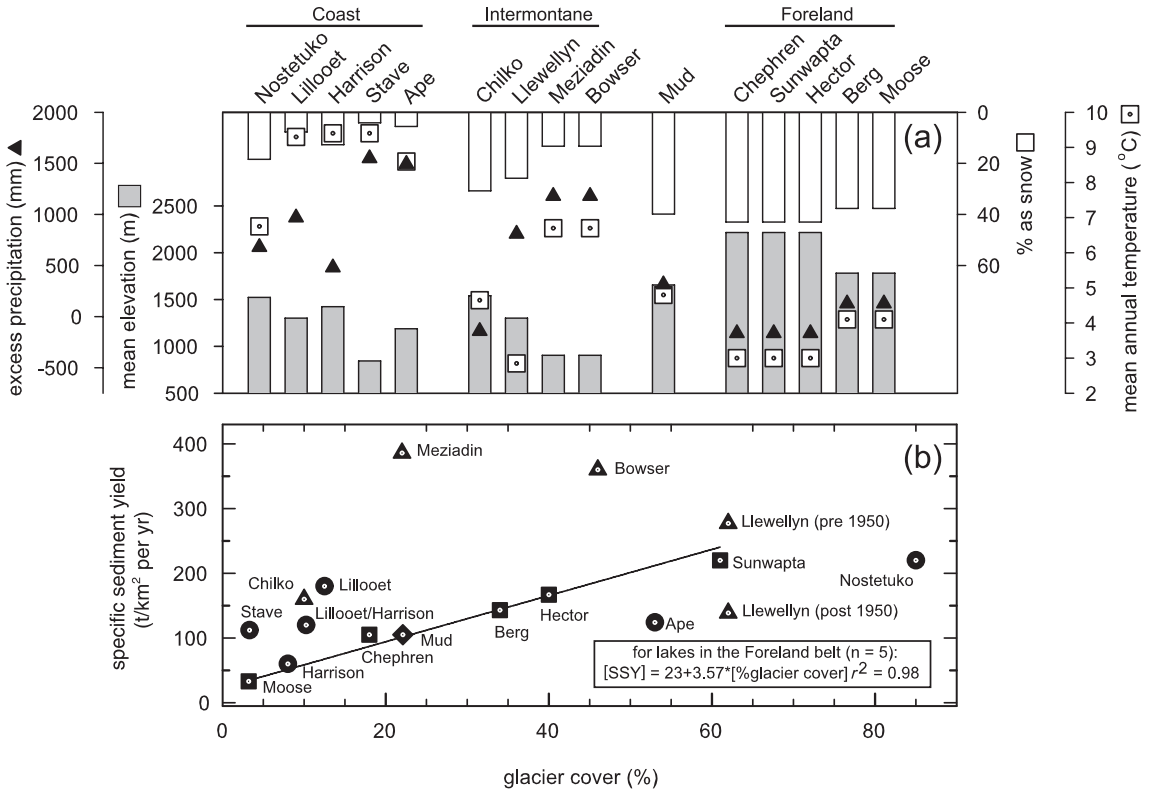

Figure 8 (a) Excess precipitation (triangles), mean area-weighted elevation (grey bars), percent precipitation received as snow (open bars) and mean annual temperature (squares) calculated using climate normals (1961–1990; Bootsma, 1997) for ecodistricts containing glacier-fed lakes in the Canadian Cordillera. Watersheds straddling ecodistrict boundaries were averaged. (b) Specific sediment yield comparison for glacier-fed lakes in the Canadian Cordillera, plotted by percent glacier cover. Tectonic belt (Figure 1) indicated using squares (Foreland belt), circles (Coast belt), triangles (Intermontane belt) and diamond (Omineca belt; Mud Lake). Lake data updated and verified from: Desloges and Gilbert (1994a, 1998), as well as Bowser Lake (Gilbert *et al*., 1997); Chilko Lake (Desloges and Gilbert, 1998); Hector Lake (Leonard, 1986); Llewellyn Inlet (Gilbert *et al*., 2006b); Meziadin Lake (Gilbert and Butler, 2004) and Sunwapta Lake (Gilbert and Shaw, 1981). Regression equation plotted for glacier-fed lakes in the carbonate-clastic Foreland belt ($n = 5$). Reprinted from Desloges and Gilbert (1998) with permission from Elsevier

buried soils in lateral moraine sequences in the Purcell Range (210 km southeast; Omineca belt) are good evidence of at least two phases of cirque glacier advance during the early part of the Neoglacial. More recently, Reyes and Clague (2004) showed five episodes of neoglacial advance at Lillooet Glacier (320 km southwest; Coast belt) including two 'Little Ice Age' episodes. Reflector geometry and sediment properties partly resolve some of this variance, but the timing and duration are difficult to refine further with the current data. However, the well-defined varves over the last 129 years clearly record the recession of glaciers from 'Little Ice Age' maxima in the upper Mud Lake drainage basin.

Finally, unlike glacier-fed lakes in the Foreland belt where lithologies are dominated by limestone, dolomite and siliclastic sedimentary rocks (Höy *et al*., 1994), sediment yield to Mud Lake is partly controlled by the erodibility of the dominant metamorphic and subdominant sedimentary lithologies. Regional climate and climate variability are also important. Understanding spatial variations in sediment yield from glacier-fed lakes when compared over a common interval of time helps to assess the lithological and regional climatic controls. Based on the whole-lake mean accumulation rate for the last 20-yr period, a lake-wide sediment accumulation volume can be computed. Assuming a specific density of 1.30 t/m^3 (based on twelve measurements from six cores), we estimate this is equivalent to a mean of 23.9×10^3 t/yr of fine sediment (clay, silt and some sand). This equates to a specific sediment yield of 93 t/km^2 per yr for the 257 km^2 drainage basin.

Figure 8a compares basic climatic characteristics among glacier-fed lakes of the Canadian Cordillera grouped by tectonic belt (Figure 1). The regional climate indices are derived from the ecodistricts of Bootsma (1997). Ecodistricts are area-interpolations defined using, among other variables, elevation, precipitation and temperature from Canadian climate normals (1961–1990). Ecodistricts are used instead of local climatic records because they provide a consistent means to compare the regional climates in which the lakes are situated; although there are limitations to the climate data synthesis by Bootsma (1997) (eg, exclusion of climate data from the highest elevations). Lakes in the colder, higher-elevation and drier Foreland belt exhibit more uniform climates than lakes in the warmer, lower-elevation and wetter Coast and Intermontane belts. The climate of the Mud Lake district most closely resembles climates of Foreland belt lakes. Figure 8b shows specific sediment yield for the same lakes inferred from lake-wide average accumulation rates (20–50 yr averages for most). Specific sediment yield is plotted against percent glacier cover in the contributing basin. Percent glacier cover is a simple index of potential sediment production by glaciers. The plot is further subdivided by tectonic belt (Figure 1) and Mud Lake is also plotted for comparison.

Glacier-fed lakes throughout the Cordillera receive from 33 to 386 t/km^2 per yr of sediment (Figure 8b). Lake records in the Foreland belt show a consistent pattern of increasing specific sediment yield with increasing glacier cover (33 to 220 t/km^2 per yr; Figure 8b). Thus, for lakes situated in this tectonic belt and climate region, glacier cover is a good predictor of specific sediment yield. Although the number of lakes used to estimate sediment yield in this region is limited ($n = 5$), the strong linear fit suggests the potential for developing a robust transfer function for lakes in this region, relating glacier coverage to sediment yield. Figure 8b shows that Mud Lake fits the generalized pattern of sediment yield versus glacier cover found in the Foreland belt despite being situated in a different geologic setting (Höy *et al*., 1994). This result is consistent with the interpretation that climate is a more dominant control on sediment yield than lithology.

The greatest variability in specific sediment yield occurs in lakes of the Coast (60 to 220 t/km^2 per yr) and Intermontane belts (138 to 386 t/km^2 per yr). Thus, for lakes situated in the more variable climates and geologic settings of these tectonic belts, glacier cover alone is not a good predictor of specific sediment yield. Lakes of similar climate (eg, Meziadin and Bowser; Figure 8a) show similar high specific sediment yield despite almost a 50% difference in glacier cover (Figure 8b). Conversely, lakes of similar glacier cover (eg, Harrison and Chilko) show different sediment yields. We know for these regions that factors other than glacier extent include: very sharp climatic gradients (from maritime to semi-arid); nival- and rainstorm-generated floods (Church, 1980; Gilbert *et al*., 2006a), a complex lithology (Höy *et al*., 1994) including Holocene volcanic activity (eg, Friele *et al*., 2005); and highly variable amounts of late Pleistocene glacio-fluvial and glacio-lacustrine sediments stored in tributary valleys (eg, Schiefer *et al*., 2001).

Conclusions

(1) Mud Lake provides a continuous record of lateglacial and Holocene sediment accumulation patterns. Accumulation rates from coarse resolution dating match the pattern reconstructed from regional moraine chronologies and show higher accumulation rates and more variable inputs early in the Holocene, a subsequent middle Holocene decline, followed by a Neoglacial increase – particularly during the 'Little Ice Age' recession phase of the last 100 years.

(2) The continuous nature of the accumulation record also provides much higher resolution of the variability in sediment delivery, which shows renewal of glacial activity during the late Neoglacial led to variable processes of sediment delivery to the lake reflective of discharge regimes controlled by snow and ice melt. Renewed sediment input follows closely the pattern of glacier expansion and the most recent varve deposits match recession from 'Little Ice Age' maximums.

(3) The stratigraphic evidence from cores correlates with lake-wide acoustic profiles and helps verify that the Holocene core record is representative of lake-wide processes and accumulation rates. The acoustic results show an early dominance of parallel-stratified sediment interpreted to be deposition in a high energy, glacially proximal environment dominated by turbidity currents. Reduced meltwater and sediment availability during the Hypsithermal, combined with stabilization of terrestrial sediments by vegetation expansion during the early Holocene, led to deposition of a thinner, concordant acoustic package via overflow or interflow currents. Subsequent deposition of thicker, concordant, parallel-stratified sediment (via overflow or interflow currents) marks renewed glacial activity (particularly in the late Neoglacial), and a likely shift in the discharge regime to higher and more variable flows, and overall increased rates of accumulation in Mud Lake.

(4) Percent glacier cover is a good predictor of specific sediment yield in lakes of the Foreland belt and the estimate of 93 t/km^2 per yr for Mud Lake lies closely within the range of specific sediment yield inferred from glacier-fed lakes of the Foreland belt. More lake chronologies are needed to better constrain variance. The more uniform climates and lithology of the lakes in the Foreland belt produce lower overall variance

in specific sediment yield for a given percent glacier cover. The more variable climates and lithology of lakes in the Intermontane and Coast belts are reflected in greater variance in specific sediment yield for a given glacier cover. A more refined analysis is needed to assess the role of climate, lithology and a range of other factors. However, we suspect climate to be the most important, especially when glacier-derived sediments are abundantly available.

Acknowledgements

This work was supported by equipment and discovery grants from the Natural Sciences and Engineering Research Council of Canada to J.R. Desloges and to R. Gilbert. The authors gratefully acknowledge field and/or laboratory assistance from K. Buckeridge, D. Mazzuchi and B. Wohlfarth and tephra analysis by J. Westgate. We thank N. Smith and J. Mason for constructive comments on this paper.

References

Alley, N.F. 1980: Holocene and latest Pleistocene cirque glaciations in the Shuswap Highland, British Columbia – discussion. *Canadian Journal of Earth Sciences* 17, 797–98.

Blais, J.M., Kalff, J., Cornett, R.J. and **Evans, R.D.** 1995: Evaluation of ^{210}Pb dating in lake sediments using stable Pb, Ambrosia pollen, and ^{137}Cs. *Journal of Paleolimnology* 13, 169–78.

Bootsma, A. 1997: Canadian ecodistrict climate normals, 1961–1990. Agriculture and Agri-Food Canada. Retrieved 13 December 2005 from http://sis.agr.gc.ca/cansis/nsdb/ecostrat/district/climate.html

Bronk Ramsey, C. 1995: Radiocarbon calibration and analysis of stratigraphy: the OxCal program. *Radiocarbon* 37, 425–30.

—— 2001: Development of the radiocarbon program OxCal. *Radiocarbon* 43, 355–63.

Chikita, K.A., Smith, N.D., Yonemitsu, N. and **Perez-Arlucea, M.** 1996: Dynamics of sediment-laden underflows passing over a subaqueous sill; glacier-fed Peyto Lake, Alberta, Canada. *Sedimentology* 43, 865–75.

Church, M. 1980: Records of recent geomorphological events. In Cullingford, R.A., Davidson, D.A. and Lewin, J., editors, *Timescales in geomorphology*. John Wiley & Sons Ltd, 13–29.

Dean, W.E. 1974: Determination of carbonate and organic matter in calcareous sediments and sedimentary rocks by loss on ignition: comparison with other methods. *Journal of Sedimentary Petrology* 44, 242–48.

Desloges, J.R. 1999: Geomorphic and climatic interpretations of abrupt changes in glaciolacustrine deposition at Moose Lake, British Columbia, Canada. *Geologiska föreningens i Stockholm förhandlingar* 121, 202–207.

Desloges, J.R. and **Gilbert, R.** 1994a: The record of extreme hydrological and geomorphological events inferred from glaciolacustrine sediments. In Olive, L.J., Loughran, R.J. and Kesby, J.A., editors, *Variability in stream erosion and sediment transport*. IAHS Publication 224, 133–42.

—— 1994b: Sediment source and hydroclimatic inferences from glacial lake sediments: the postglacial sedimentary record of Lillooet Lake, British Columbia. *Journal of Hydrology* 159, 375–93.

—— 1995: The sedimentary record of Moose Lake: implications for glacier activity in the Mount Robson area, British Columbia. *Canadian Journal of Earth Sciences* 32, 65–78.

—— 1998: Sedimentation in Chilko Lake: a record of the geomorphic environment of the eastern Coast Mountains of British Columbia, Canada. *Geomorphology* 25, 75–91.

Duford, J.M. and **Osborn, G.D.** 1978: Holocene and latest Pleistocene cirque glaciations in Shuswap Highland, British Columbia. *Canadian Journal of Earth Sciences* 15, 865–73.

—— 1980: Holocene and latest Pleistocene cirque glaciations in the Shuswap Highland, British Columbia – reply. *Canadian Journal of Earth Sciences* 17, 799–800.

Eyles, N. and **Mullins, H.T.** 1997: Seismic-stratigraphy of Shuswap Lake, British Columbia, Canada. *Sedimentary Geology* 109, 283–303.

Eyles, N., Boyce, J.I., Halfman, J.D. and **Koseoglu, B.** 2000: Seismic stratigraphy of Waterton Lake: a sediment starved glaciated basin in the Rocky Mountains of Alberta, Canada and Montana, USA. *Sedimentary Geology* 130, 283–311.

Fisher, T.G. 2004: Vibracoring from lake ice with a lightweight monopod and piston coring apparatus. *Journal of Paleolimnology* 31, 377–82.

Friele, P.A., Clague, J.J., Simpson, K. and **Stasiuk, M.** 2005: Impact of a Quaternary volcano on Holocene sedimentation in Lillooet River valley, British Columbia. *Sedimentary Geology* 176, 305–22.

Fulton, R.J. 1984: Quaternary glaciation, Canadian Cordillera. In Fulton, R.J., editor, *Quaternary stratigraphy of Canada – a Canadian contribution to IGCP Project 24*. Geological Survey of Canada, Paper 84-10, 39–48.

Gilbert, R. and **Butler, R.** 2004: The physical limnology and sedimentology of Meziadin Lake, Northern British Columbia, Canada. *Arctic, Antarctic and Alpine Research* 36, 33–41.

Gilbert, R. and **Shaw, J.** 1981: Sedimentation in proglacial Sunwapta Lake, Alberta. *Canadian Journal of Earth Sciences* 18, 81–93.

Gilbert, R. and **Desloges, J.R.** 1992: The late Quaternary sedimentary record of Stave Lake, southwestern British Columbia. *Canadian Journal of Earth Sciences* 29, 1997–2006.

Gilbert, R., Desloges, J.R. and **Clague, J.J.** 1997: The glacilacustrine sedimentary environment of Bowser Lake in the northern Coast Mountains of British Columbia, Canada. *Journal of Paleolimnology* 17, 331–46.

Gilbert, R., Crookshanks, S., Hodder, K.R., Spagnol, J. and **Stull, R.B.** 2006a: The record of an extreme flood in the sediments of montane Lillooet Lake, British Columbia: implications for paleoenvironmental assessment. *Journal of Paleolimnology*.

Gilbert, R., Desloges, J.R., Lamoureux, S.F., Serink, A. and **Hodder, K.R.** 2006b: The geomorphic and paleoenvironmental record in sediments of Atlin Lake, northern British Columbia. *Geomorphology*.

Hallett, D.J., Hills, L.V. and **Clague, J.J.** 1997: New accelerator mass spectrometry radiocarbon ages for the Mazama tephra layer from Kootenay National Park, British Columbia, Canada. *Canadian Journal of Earth Sciences* 34, 1210–19.

Hamblin, P.F. and **Carmack, E.C.** 1978: River-induced currents in a fjord lake. *Journal of Geophysical Research* 83, 885–99.

Höy, T., Church, B.N., Legun, A., Glover, K., Gibson, G., Grant, B., Wheeler, J.O., Dunne, K.P.E., Cunningham, J. and **Desjardins, P.J.** 1994: *The geology of the Kootenay Mineral Assessment Region*. British Columbia Ministry of Energy, Mines and Petroleum Resources, Open File 1994-8.

Karlstrom, E.T. and **Osborn, G.** 1992: Genesis of buried paleosols and soils in Holocene and late Pleistocene tills, Bugaboo Glacier area, British Columbia, Canada. *Arctic and Alpine Research* 24, 108–23.

Leonard, E.M. 1986: Varve studies at Hector Lake, Alberta, Canada and the relationship between glacial activity and sedimentation. *Quaternary Research* 25, 199–214.

Leonard, E.M. and **Reasoner, M.A.** 1999: A continuous Holocene glacial record inferred from proglacial lake sediments in Banff National Park, Alberta, Canada. *Quaternary Research* 51, 1–13.

Luckman, B.H., Harding, K.A. and **Hamilton, J.P.** 1987: Recent glacier advances in the Premier Range, British Columbia. *Canadian Journal of Earth Sciences* 24, 1149–61.

Marczak, W. 1997: Water as a standard in the measurements of speed of sound in liquids. *Journal of the Acoustical Society of America* 102, 2776–79.

Osborn, G. and **Luckman, B.H.** 1988: Holocene glacier fluctuations in the Canadian Cordillera (Alberta and British Columbia). *Quaternary Science Reviews* 7, 115–28.
Pickrill, R.A. and **Irwin, J.** 1983: Sedimentation in a deep glacier-fed lake – Lake Tepako, New Zealand. *Sedimentology* 30, 63–75.
Reimer, P.J., Baillie, M.G.L., Bard, E., Bayliss, A., Beck, J.W., Bertrand, C.J.H., Blackwell, P.G., Buck, C.E., Burr, G.S., Cutler, K.B., Damon, P.E., Edwards, R.L., Fairbanks, R.G., Friedrich, M., Guilderson, T.P., Hogg, A.G., Hughen, K.A., Kromer, B., McCormac, F.G., Manning, S.W., Ramsey, C.B., Reimer, R.W., Remmele, S., Southon, J.R., Stuiver, M., Talamo, S., Taylor, F.W., van der Plicht, J. and **Weyhenmeyer, C.E.** 2004: IntCal04 terrestrial radiocarbon age calibration, 26–0 ka BP. *Radiocarbon* 46, 1029–58.
Reyes A.V. and **Clague J.J.** 2004: Stratigraphic evidence for multiple Holocene advances of Lillooet Glacier, southern Coast Mountains, British Columbia. *Canadian Journal of Earth Sciences* 41, 903–18.
Schiefer, E., Slaymaker, O. and **Klinkenberg, B.** 2001: Physiographically controlled allometry of specific sediment yield in the Canadian Cordillera: a lake sediment-based approach. *Geografiska Annaler* 83A, 55–65.
Schnurrenberger, D.W., Russell, J.M. and **Kelts, K.R.** 2003: Classification of lacustrine sediments based on sedimentary components. *Journal of Paleolimnology* 29, 141–54.
Smith, D.G. 1998: Vibracoring: a new method for coring deep lakes. *Palaeogeography, Palaeoclimatology, Palaeoecology* 140, 433–40.
Smith, N.D., Venol, M.A. and **Kennedy, S.K.** 1982: Comparison of sedimentation regimes in four glacier-fed lakes of western Alberta. In Davidson-Arnott, R., Nickling, W. and Fahey, B.D., editors, *Research in glacial, glacio-fluvial and glacio-lacustrine systems.* University of Guelph, 203–38.
Vogel, J.S., Cornell, W., Nelson, D.E. and **Southon, J.R.** 1990: Vesuvius/Avellino, one possible source of seventeenth century BC climatic disturbances. *Nature* 344, 534–37.
Weirich, F. 1986: The record of density-induced underflows in a glacial lake. *Sedimentology* 33, 261–77.
Wheeler, J.O. and **McFeely, P.** 1991: *Tectonic assemblage map of the Canadian Cordillera and adjacent parts of the United States of America*. Geological Survey of Canada Map 1712A.
Wright, R.F. and **Nydegger, P.** 1980: Sedimentation of detrital particulate matter in lakes: influence of currents produced by inflowing rivers. *Water Resources Research* 16, 597–601.